Briefing Space Weather

2022/06/13

1 Sun

1.1 Responsible: José Cecatto

06/06 – No flare (M/X); No fast wind stream; 2 CME c.h.c. toward the Earth;
06/07 – No flare (M/X); No fast wind stream; 5 CME c.h.c. toward the Earth;
06/08 – No flare (M/X); No fast wind stream); 1 CME c.h.c. toward the Earth;
06/09 – No flare (M/X); No fast wind stream; 2 CME c.h.c. toward the Earth;
06/10 – 1 M-1 flare; No fast wind stream; 3 CME c.h.c. toward the Earth;
06/11 – No flare (M/X); No fast wind stream; 2 CME c.h.c. toward the Earth;
06/12 – No flare (M/X); Fast wind stream (=< 500 km/s); No CME toward the Earth;
06/13 – 1 M-3.5 flare, type-II burst, shortwave radio blackout; Fast wind stream (=< 550 km/s); 5 CME c.h.c. toward
the Earth;
Prev.: Fast wind stream up to June 16; for the next 2 days low (25% M, 05% X) probability of M / X flares; also,
occasionally other CME can present component toward the Earth.
c.h.c. – can have a component; * partial halo; ** halo

2 Interplanetary Medium

2.1 Responsible: Paulo Jauer

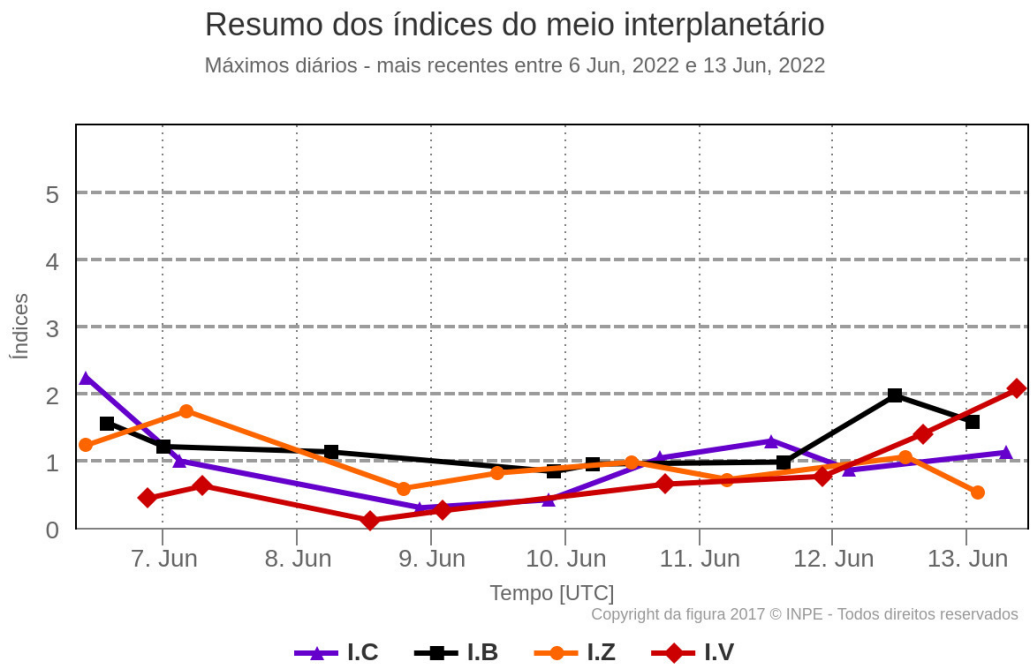

- The interplanetary medium region in the last week showed a low/moderate level of plasma perturbations due to the possible interaction of CME and HSS-like structures identified by the DISCOVR satellite in the interplanetary medium.
- The modulus of the interplanetary magnetic field component showed 1 maximum peak on June 12 at 11:30 at ∼14.85 nT.
- The BxBy components showed variations in the analyzed period, both remaining oscillating within the [+12.5, -12.5] nT interval, with the presence of a sector change on June 11 at 06:30 UT.
- The component of the bz field showed fluctuations oscillating mostly around negative values. The bz component showed an abrupt variation of ∼ -6.84 nT on June 6th at 09:30 due to the interaction of an ICME.
- The solar wind density peaked on June 6 at 10:30 am at 42.6 p/cm^3. The density remained oscillating below 27 p/cm^3 for the rest of the period.
- The solar wind speed had fluctuated decreasing throughout the week, with a minimum value on June 6 at 8:30 am of 263 km/s and a maximum value at 9:30 am on June 13 of 532 km/s.
- The position of the magnetopause was oscillating on average around the equilibrium position. On July 6th at 10:30 am, it presented a maximum compression of 8,014 Re.

3 Radiation Belts

3.1 Responsible: Ligia Alves da Silva

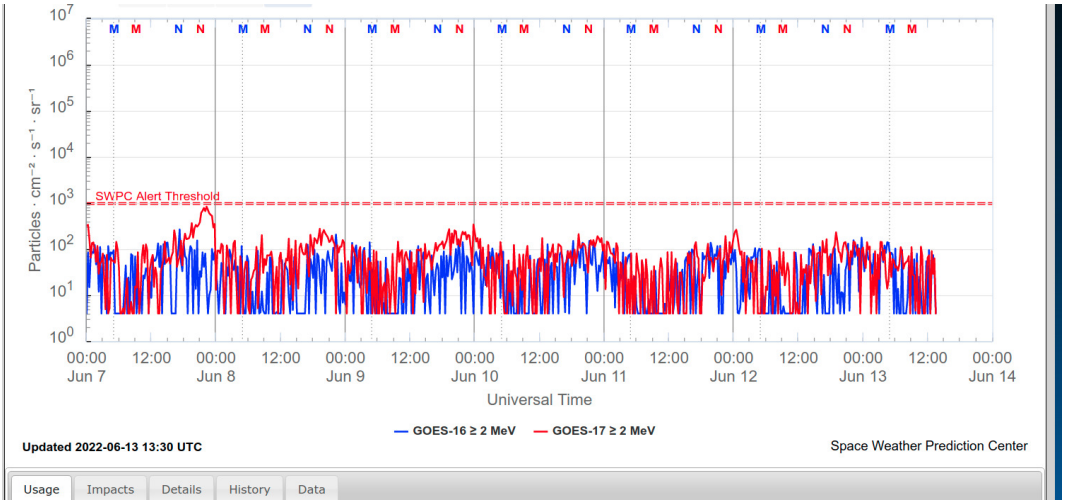

Figura 1: High-energy electron flux (> 2MeV) obtained from GOES-16 and GOES-17 satellite. Source: `https://www.swpc.noaa.gov/products/goes-electron-flux`

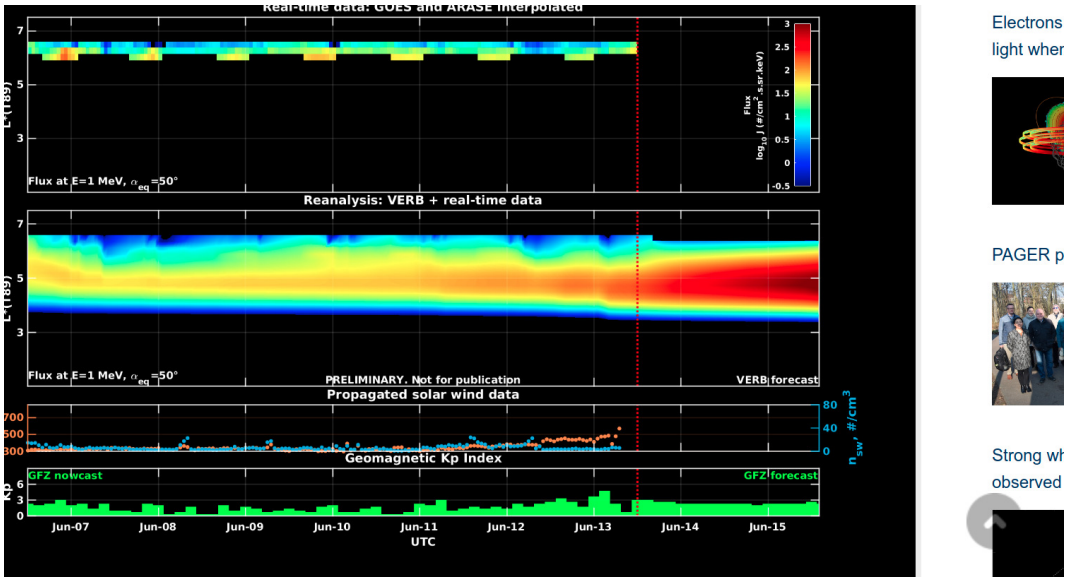

Figura 2: high-energy electron flux data (real-time and interpolated) obtained from ARASE, GOES-16, GOES-17 satellites. Reanalysis's data from VERB code and interpolated electron flux. Solar wind velocity and proton density data from ACE satellite. Source: `https://rbm.epss.ucla.edu/realtime-forecas`

High-energy electron flux (>2 MeV) in the outer boundary of the outer radiation belt obtained from geostationary satellite data GOES-16 and GOES-17 (Figure 1) is below 10^2 particles/$(cm^2 ssr)$ during almost the entire analyzed period, showing only an electron flux increase at the end of the June 7th, which reached 103 particles/(cm2 s sr) in a short period of time.

The GOES-16, GOES-17, and Arase satellite data are analyzed and interpolated to observe the high-energy electron flux variability (1 MeV) in the outer radiation belt (Figure 2). Additionally, the VERB code rebuilds this electron considering the Ultra Low Frequency (ULF) waves' radial diffusion. The simulation (VERB code) shows that the electron flux varies at the outer boundary of the outer radiation belt. The electron flux increase occurred concomitantly with the ULF wave activities.

4 ULF waves

4.1 Responsible: Graziela B. D. Silva

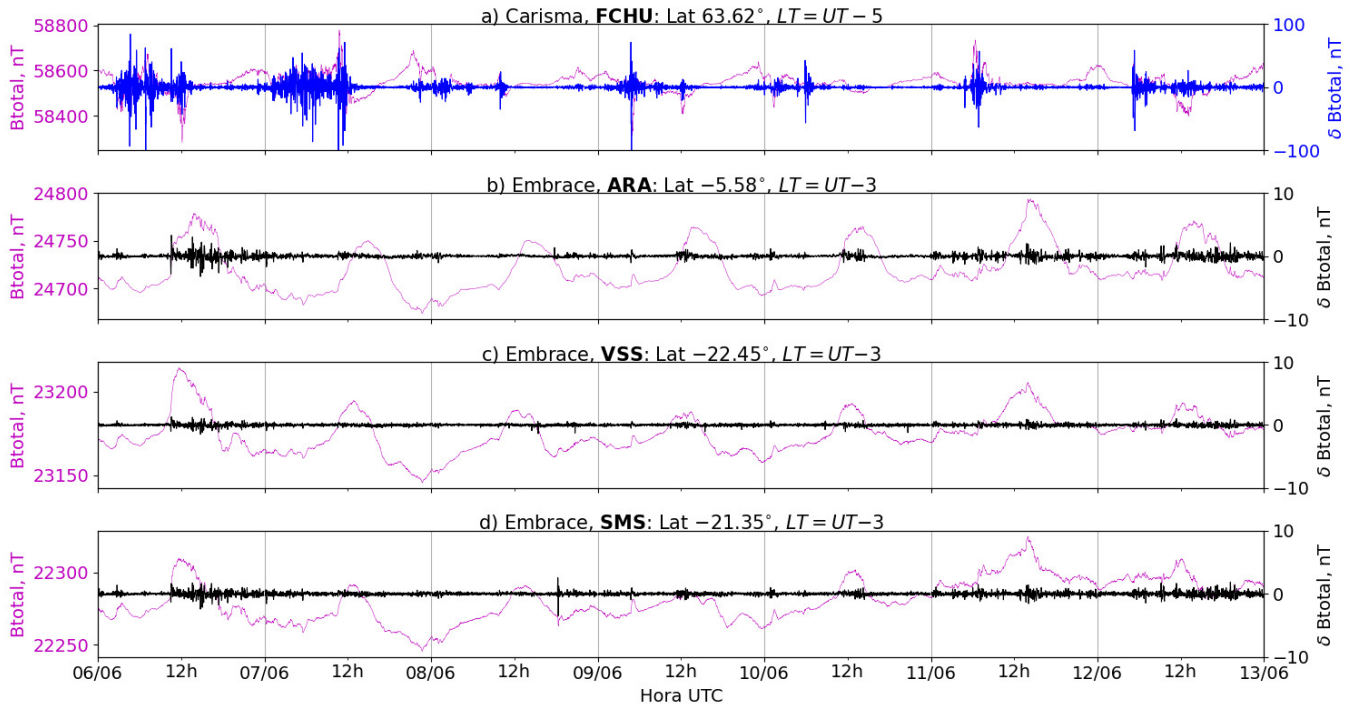

Figura 3: a) Timeseries of the geomagnetic field total component measured at FCHU station (Fort Churchill) of the CARISMA magnetometer network in magenta, along with the associated perturbation in the Pc5 band shown in blue. b-d) timeseries of the geomagnetic field total component measured at stations ARA (Araguatins), VSS (Vassouras) and SMS (São Martinho da Serra) of the EMBRACE network in magenta, along with the Pc5 perturbation in blue.

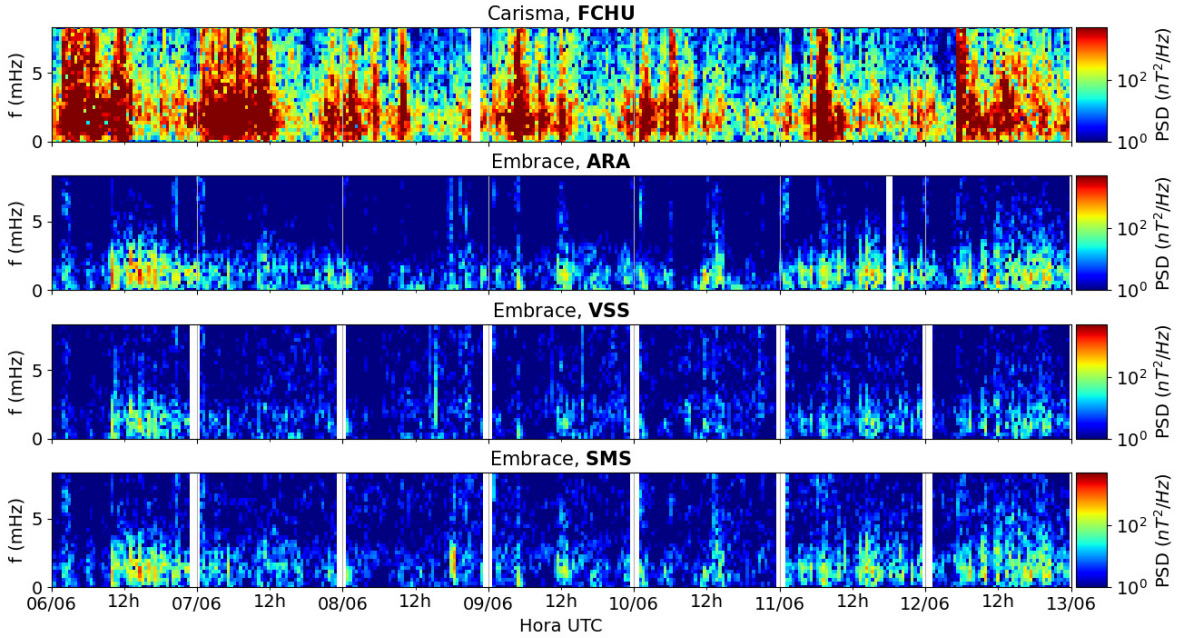

Figura 4: a-d) Time evolution of the power spectral density obtained from the filtered timeseries of the geomagnetic field total component (δ Btotal) for a) the high latitude station (FCHU-CARISMA), and b-d) for the low latitude stations of EMBRACE (ARA, VSS, SMS).

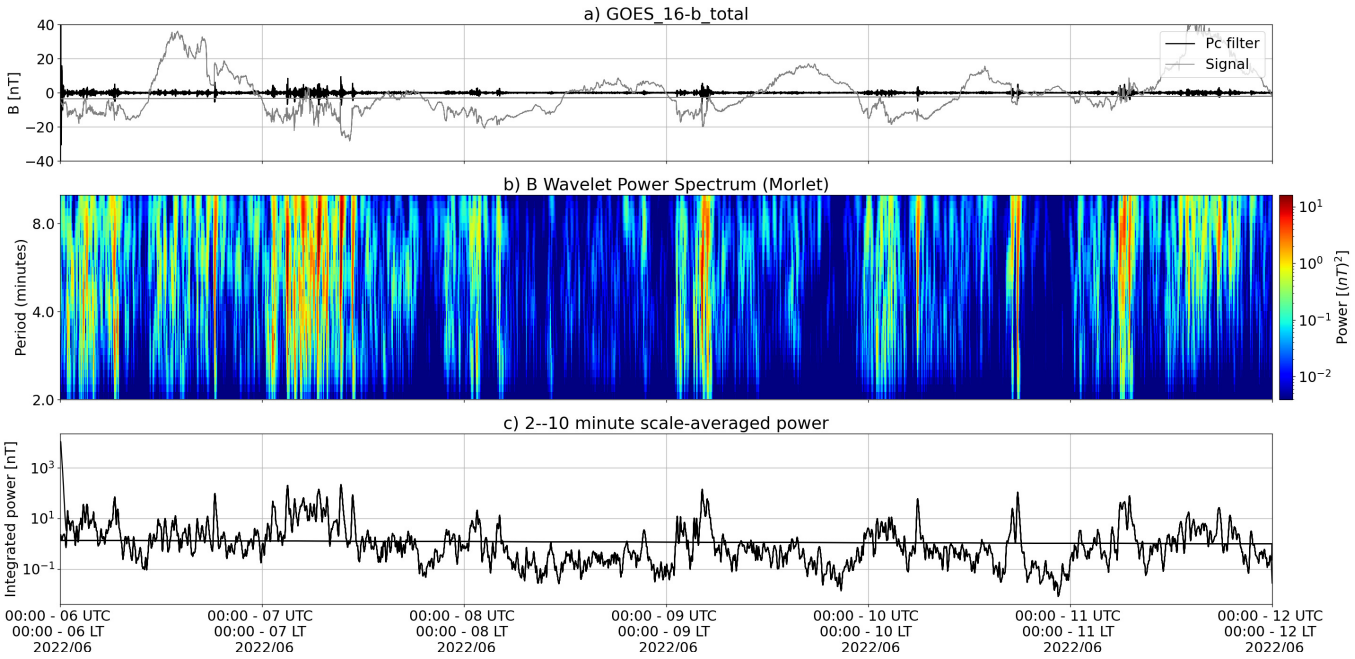

Figura 5: a) Timeseries of the geomagnetic field total component measured by GOES 16, together with the Pc5 fluctuation in black. b) Wavelet power spectrum of the filtered timeseries. c) Average ULF power in the period range from 2 to 10 minutes.

- There was intense and continuous activity of Pc5 ULF waves between 06/june and 07/june, as measured by GOES 16 at geosynchronous orbit (L $\sim$ 6.6). The wave activity was associated with the arrival of an ICME (interplanetary coronal mass ejection) on 06/june.

- For the ground-based stations, an intense activity of ULF waves was registered on 06/june in Fort Churchill (FCHU/high latitude) up to 12 UT, while at the EMBRACE stations the main activity started from ∼ 12 UT with the arrival of the interplanetary shock. Such activity persisted through the rest of the day.
- On 07/june, the ULF wave activity persisted in FCHU, but not for the EMBRACE stations.
- Through 08-10/june, there was weak to moderate activity of the waves both in the auroral and equatorial regions, although in FCHU it was less continuos.
- Through 11-12/june, we highlight the constinous activity of ULF waves at the EMBRACE stations, possibly due to the gradual increase in the solar wind velocity.

5 Ondas EMIC

5.1 Responsible: Claudia Medeiros

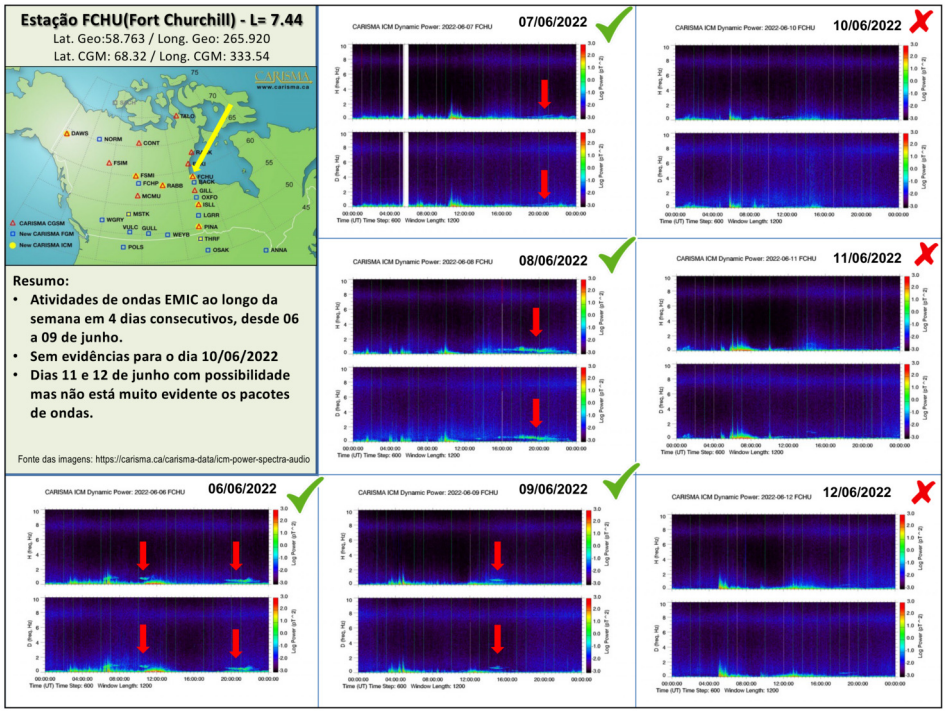

6 Geomagnetic activity

6.1 Responsible: Lívia Alves

In the week of 07-13 June, the following events related to geomagnetic activity stand out:

- The data from the Embrace magnetometer network showed instabilities throughout the period, with emphasis on Jun 7, 11 and 13 - The magnetometers of the Embrace network recorded a drop followed by an enhancement in the H component.
- The geomagnetic activity was unstable throughout the period, the AE index was unsettled in the period, AE index reached 1000 nT. The Dst index ranged from +22 nT to -5 nT. The highest Kp of the week was 5-.
- The gemagnetic field measured at the GOES orbit shows instabilities on 07 and 11-June.

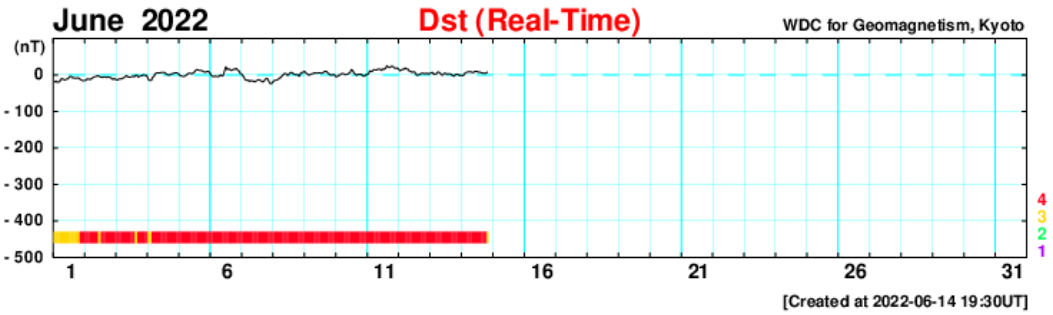

Figura 6: Time evolution of the geomagnetic Dst index.

7 Ionosphere

7.1 Responsible: Laysa Resende

Boa Vista:

- There were not occurred spread F during this week.
- The Es layers reached scale 2 during this week.

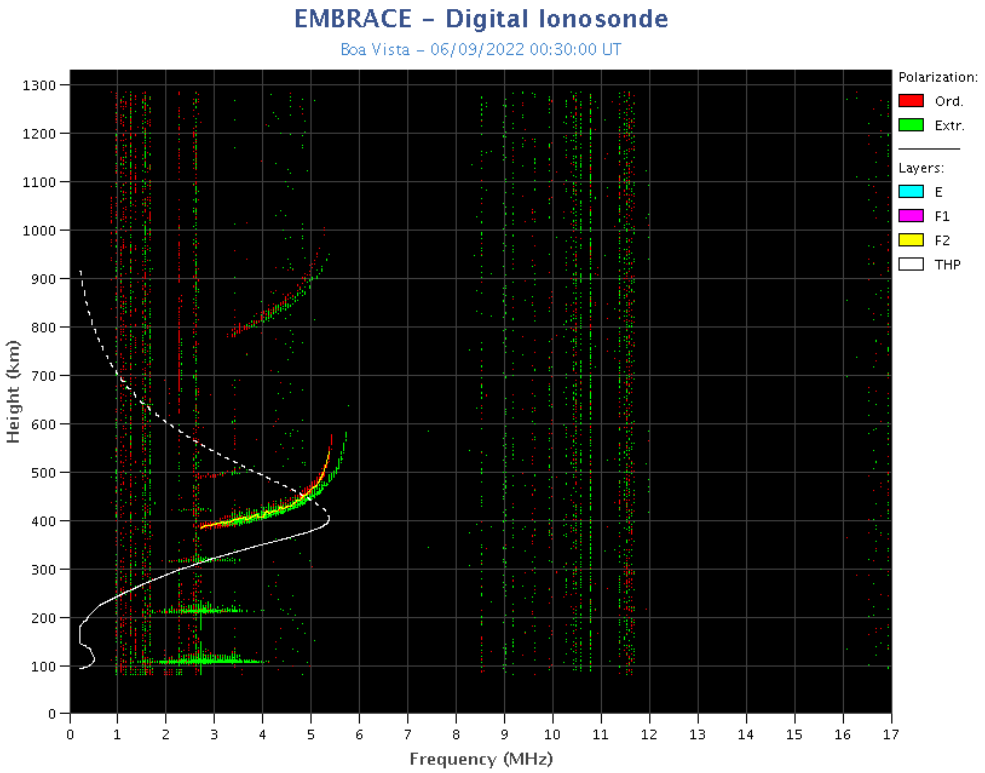

Cachoeira Paulista:

- There were not occurred spread F during this week.
- The Es layers reached scale 2 during this week.

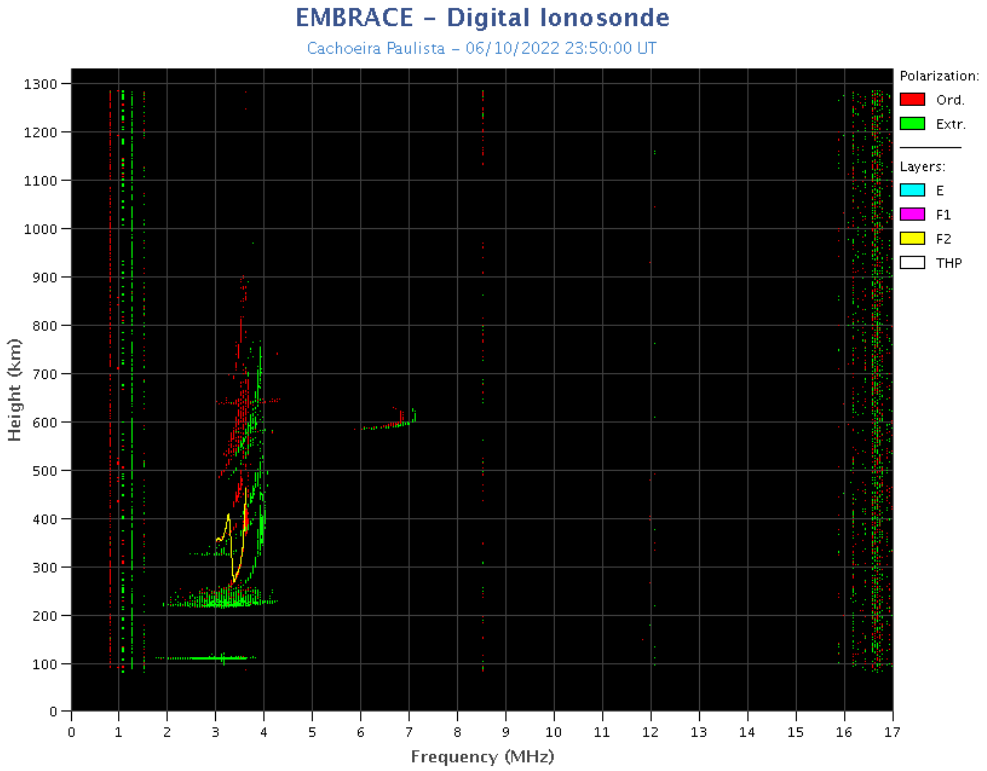

São Luís:

- There were a weak spread F during this week.
- The Es layers reached scale 4 on day 06.

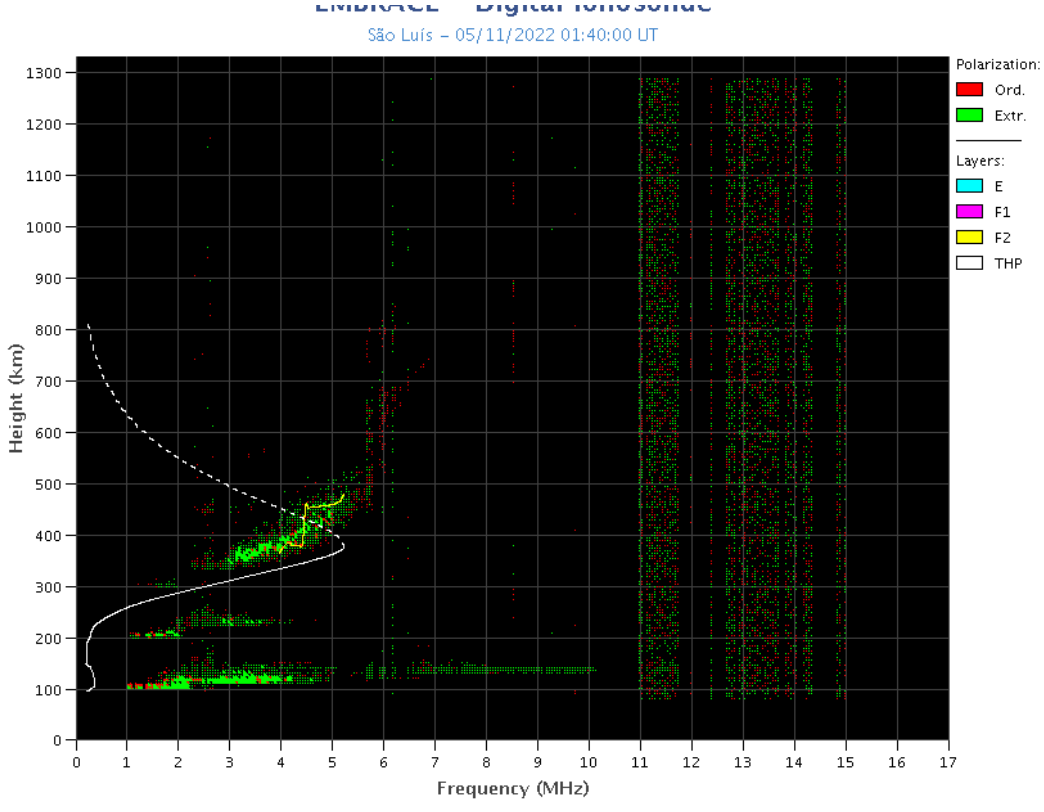

8 Scintilation

8.1 Responsible: Siomel Savio Odriozola

In this report on the S4 scintillation index, data from SLMA in São Luiz/MA, STSN in Sinop/MT, UFBA in Bahia/BA and SJCE in São José dos Campos/SP are presented. The S4 index tracks the presence of irregularities in the ionosphere having a spatial scale $\sim$ 360 m. This week, data availability was only until 06/09 in all the stations. The SLMA and SJCE stations showed S4 values below 0.2 throughout the week. STSN station showed weak scintillation values on 06/06 around the same time reported the previous week (Figure 1 upper panel). Small scintillation was recorded at UFBA during the early hours of 06/06, 07 and 09(Figure 1 lower panel). The behavior of the UFBA station is very similar to what was observed the previous week.

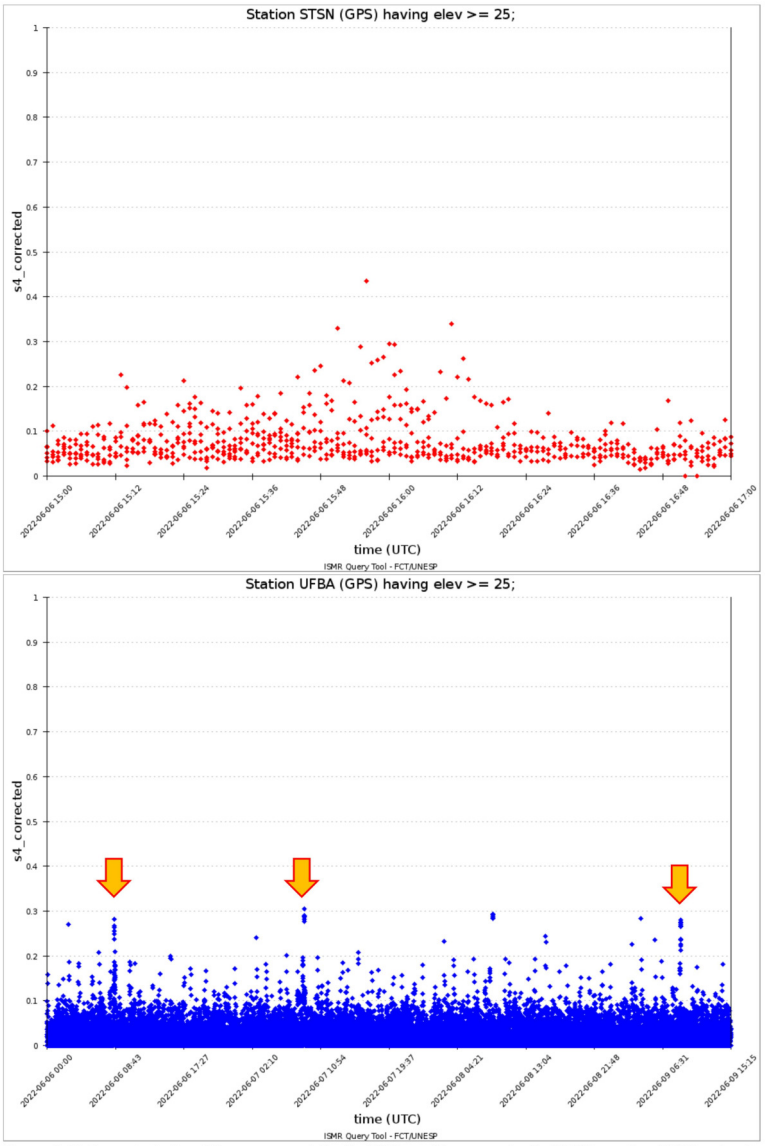

Figura 1: Valores do índice S4 para a constelação GPS medidos na estação STSN no dias 06/06 entre ás 1500UT e ás 17 (painel superior). O painel inferior mostra os valores do S4 medidos em UFBA entre os dias 06—09/06.

9 All-Sky Imager

9.1 Responsible: LUME

All-Sky Imager EPBs Observation
Observações das EPBs por meio do imageador All-Sky
June 05 - June 11, 2022 || 05 de junho - 11 de junho, 2022

Observatory Observatório	June 05 junho 05	June 06 junho 06	June 07 junho 07	June 08 junho 08	June 09 junho 09	June 10 junho 10	June 11 junho 11
CA	✗	✗	✗	✓	✓	✓	✓
BJL	✗	✗	✗	✗	✗	✗	✗
CP	✓	✓	✓	✓	✓	✓	✓
SMS	✓	✗	✗	✗	✓	✓	✓

Definition of Symbols	
CA	São João do Cariri
BJL	Bom Jesus da Lapa
CP	Cachoeira Paulista
SMS	São Martinho da Serra
✓	Observation - Observação
✗	No Observation - Sem Observação
❍	Clear sky - Céu limpo
	Partly Cloudy - Parcialmente Nublado
	Cloudy - Nublado

- At the Sao Joao do Cariri observatory no geophysical phenomena such as plasma bubbles and traveling ionospheric disturbances were observed during the period. On days 5, 6 and 7, there were no observations.
- At the Bom de Jesus da Lapa observatory there was no observation due to technical problems.
- At the Cachoeira Paulista observatory no geophysical phenomena such as plasma bubbles and traveling ionospheric disturbances were observed during the period. The sky was cloudy throughout the week.
- Finally, at the observatory of Sao Martinho da Serra observatory, no geophysical phenomena such as plasma bubbles and traveling ionospheric disturbances were observed during the period. On days 5, 6 and 7, there were no observations.

TEC

- No plasma bubbles were observed during the entire period. Besides, the equatorial anomaly was observed every day.